# *CHANDRA* OBSERVATIONS OF THE GALACTIC CENTER AND NEARBY EDGE-ON GALAXIES

**Q. Daniel Wang**

Department of Astronomy, University of Massachusetts, Amherst, MA 01003, USA

arXiv:astro-ph/0202317v1 17 Feb 2002

Abstract

I review our recent *Chandra* surveys of the center region of the Milky Way and other nearby edge-on galaxies. Our Galactic center survey, consisting of 30 overlapping pointings, provides an unprecedented high-resolution, broad-band X-ray view of a 0.8x2 square degree swath along the Galactic plane. This X-ray panorama allows a separation of the discrete source and diffuse X-ray components. Our preliminary analysis has led a detection of about 1000 discrete sources. Less than 20 of these sources are previously known objects, most of which are bright X-ray binaries. We find that the diffuse X-ray emission dominates over the contribution from faint discrete sources and is globally associated with distinct interstellar structures observed at radio and mid-infrared wavelengths. We study how high-energy activities in the center region affect the immediate vicinity and may influence other aspects of the Galaxy.

We have further observed nearby edge-on late-type disk galaxies in fields of low foreground Galactic extinction to gain external perspectives of the global disk/halo interaction. We have detected a giant diffuse X-ray-emitting corona around the galactic disk of NGC 4631. Extraplanar diffuse X-ray emission is also detected around NGC 3556. These X-ray-emitting coronae morphologically resemble the radio halos of these galaxies, indicating a close connection between outflows of hot gas, cosmic rays, and magnetic field from the galactic disks. There is only marginal evidence for extraplanar diffuse X-ray emission in NGC 4244 — a galaxy with an extremely low star formation rate. In general, the extraplanar diffuse X-ray emission is evidently related to recent massive star forming activities in the galactic disks, especially in their central regions.

Key words: Missions: *Chandra* – galaxies: individual the Milky Way, NGC 4631, NGC 4244, NGC 3556 (M108)

## 1. Introduction

It is becoming increasingly clear that galaxies are dynamic ecosystems. Especially important in shaping the structure and evolution of galaxies are high-energy activities that can generate high-velocity and high-temperature gas. We have been carrying out a systematic observing program to gain various perspectives of high-energy phenomena and processes in galaxies. We are particularly interested in studying the production, transportation, and cooling of X-ray-emitting gas.

In this presentation, I concentrate on describing our *Chandra* surveys of nearby edge-on galaxies and the center region of the Milky Way. At a distance of 8 kpc from the Sun, the Galactic center (GC) region represents the best laboratory for a detailed study of the population and nature of various discrete X-ray sources and the processes related to the gas heating and escaping in a galactic nuclear environment. Our nearby edge-on galaxy survey so far includes NGC 4631, NGC 3556, and NGC 4244, providing a global view of the galactic disk/halo interplay. But before going on to discuss these new observations, let me briefly summarize what we know about X-ray-emitting gas around disk galaxies in the pre-*Chandra* era.

## 2. Pre-*Chandra* Observations

*ROSAT* observations gave only marginal evidence for the presence of extraplanar diffuse X-ray emission in several relatively normal edge-on spirals, most noticeably NGC 4631 (Wang et al. 1995) and NGC 891 (Bregman & Houck 1997). Both the spatial resolution and the counting statistics of these observations were very limited; confusion with point-like sources was significant.

*ROSAT* studies of the diffuse soft X-ray background have led to the conclusion that large amounts of X-ray-emitting gas are also present at high Galactic latitudes and beyond the Local Bubble around the Sun (e.g., Snowden et al. 1997). Although the Galaxy-wide distribution of the hot gas is difficult to determine, it has been proposed that the GC region of the Milky Way may play an important role in supplying the hot gas (Wang 1997; Almy et al. 2000; Sofue 2000).

While the massive black hole at the dynamic center of our Galaxy is not particularly active at present (e.g., Baganoff et al. 2001), enhanced X-ray emission has been observed in the surrounding region (e.g., Koyama et al. 1996; Wang et al. 2002). The presence of various spectral lines (e.g., 6.7-keV Fe XXV K$\alpha$), as detected by *ASCA*, has been taken as an indication for large amounts of very hot diffuse gas ($\sim 10^8$ K; Koyama et al. 1996). Such hot gas cannot be confined by the gravity of the region and is likely to escape.

Proc. Symposium *'New Visions of the X-ray Universe in the XMM-Newton and Chandra Era'* 26–30 November 2001,

*Figure 1. ROSAT all sky survey map of the inner region of the Galaxy in the $\sim 1.5$ keV band (Snowden et al. 1997). The box in the middle marks the region covered by ROSAT pointed observations (Fig. 2).*

*Figure 2. A close-up of the central region of the Galaxy. The mosaic is constructed with ROSAT PSPC observations (Sidoli et al. 2001) in the highest energy band (1.5–2.4 keV; Snowden et al. 1997). The central rectangular box oriented along the Galactic plane outlines the field mapped out by our Chandra survey (Fig. 3).*

The outflow of the hot gas from the GC region may be responsible for much of the diffuse soft X-ray background, particularly in the inner field of the Galaxy. Fig. 1 shows a large-scale hollow-cone-shaped soft X-ray feature on each side of the Galactic plane. This distinct morphology resembles those seen in nearby galaxies with active nuclear star formation and suggests a hot gas outflow from the GC region of the Milky Way. A close-up of the region, as presented in Fig. 2, further shows a bright soft X-ray plume that apparently connects to the southern large-scale X-ray feature, $\gtrsim 300$ pc away from the Galactic plane at the distance of the GC (Fig. 1). The exact morphology of this plume is uncertain, because of the differential X-ray absorption across the field. A comparison of the *ROSAT* PSPC and *IRAS* 100 micron images suggests that the deficit of the soft X-ray emission between the plume and the circumnuclear region is most likely due to X-ray shadowing by foreground interstellar dusty gas. There might also be outflows from other adjacent massive star forming regions. But the plume just below the GC is the most prominent and coherent vertical diffuse soft X-ray feature observed, and it may represent the hot gas outflow from the GC region to the southern halo of the Galaxy.

## 3. *Chandra* Survey of the Galactic Center

We have carried out a *Chandra* survey of the Galactic ridge around the GC (Fig. 3; Wang et al. 2002). This survey consists of 30 separate observations, which were all taken in July 2001. A mosaic of these observations, including only the data from the ACIS-I, covers a field of $\sim 0.8^\circ \times 2^\circ$. The survey data provide an invaluable database for studying the interplay between stars, gas, dust, gravity, and magnetic fields in the unique environment of the center region.

### 3.1. Discrete sources and Features

Our preliminary analysis of the survey data, together with three deeper archival observations, has led a detection of about 1000 discrete sources (Wang et al. 2002). Less than 20 of these sources are previously known objects, most of which are bright X-ray binaries. The newly-detected sources must represent a combination of various populations, including background AGNs and foreground stars as well as X-ray binaries (CVs, accreting neutron star and black hole systems) and massive stars in the GC region, although their relative populations in the field are still very much uncertain.

The number of the detected X-ray sources in our field seems to be much higher than that expected from a measurement of the source density in a relatively blank region of the Galactic plane (Ebisawa et al. 2001). But, we are yet to quantify this source excess, taking into consideration such position-dependent parameters as the detection threshold, the line-of-sight X-ray absorption, and the local diffuse X-ray background level. The X-ray absorption, for example, clearly varies across the field, affecting the surface brightness distribution, particularly in the 1–3 keV energy band. The majority of the detected sources are in the energy range of 2–10 keV within a luminosity range of $10^{32} - 10^{35}$ ergs s$^{-1}$ at the distance of the GC.

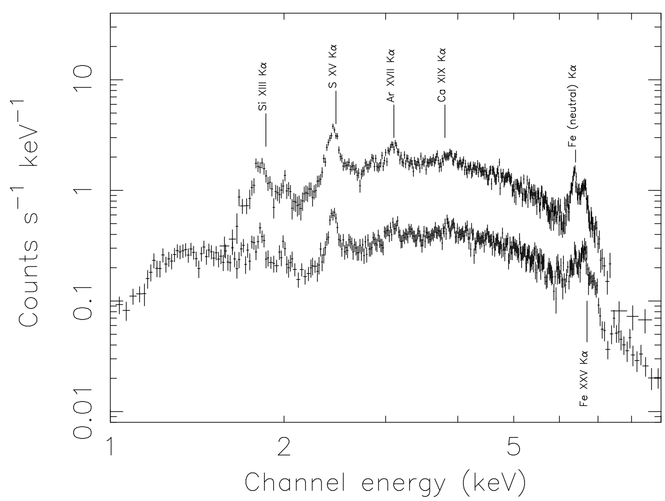


*Figure 4. Comparison of accumulated source (lower) and diffuse X-ray emission (upper) spectra for the central enhancement above the surrounding background (see text).*

Fig. 4 compares the accumulated X-ray spectra of source and diffuse components in the central region. These two spectra are extracted from an ellipse (with the major and minor axis equal to 50′ and 12′), centered on the Sgr A$^*$ and oriented along the Galactic plane. Regions around the two brightest sources (1E 1740.7-2942 and 1E 1743.1-2843) are excluded to minimize the spectral pile-up problem. A diffuse background, obtained in the outer field and normalized in both exposure and area, is subtracted from the two spectra. However, the X-ray surface brightness distribution varies strongly across the field, especially in the region close to Sgr A. Therefore, the above simple subtraction may still leave a considerable diffuse X-ray contribution (e.g., line emission) to the discrete source spectrum in Fig. 4.

*Figure 3. Chandra ACIS-I intensity map of the Galactic central ridge. This map, constructed in the 1–8 keV range, is adaptively smoothed with a signal-to-noise ratio of $\sim 3$ and is plotted logarithmically to emphasize low surface brightness emission. The saw-shaped boundaries of the map, plotted in Galactic coordinates, results from a specific roll angle of the observations.*

*Figure 5. Galactic center region across the spectrum: red: radio 90 cm (VLA; LaRosa et al. 2001); green: mid-infrared (MSX; Price et al. 2001); blue: X-ray (1–8 keV; Fig. 3)*

The total count rate from the detected discrete sources is comparable to that of the diffuse emission. But excluding the two brightest sources, the source contribution is only $\sim 20\%$ of the diffuse emission from the central enhancement. Including the subtracted X-ray background radiation, which is still uncertain, this fraction would be smaller. No known source population with $L_x < 10^{32}$ ergs s$^{-1}$ could explain the diffuse hard X-ray emission as observed.

Our ongoing study of the X-ray spatial, spectral, and timing properties as well as counterparts in other wavelength bands will help us to constrain the nature of individual sources. Here I describe two examples of interesting X-ray sources and features that we have been studying.

#### 3.1.1. Arches cluster and its vicinity

*Figure 6. ACIS-I 1–7 keV intensity contours overlaid on the HST NICMOS 1.6 micro image of the Arches cluster (Figer et al. 1999). The contours are at 26, 32, 44, 68, 120, 220, 420, 820, and 1620* $\times 10^{-3}$ counts s$^{-1}$ arcmin$^{-2}$.

The Arches cluster is the most compact massive star cluster known in our Galaxy. The cluster was covered by one of our survey observations in a position that is significantly closer to the telescope axis than the *Chandra* Cycle 1 image presented by Yusef-Zadeh et al. (2002). We find that the X-ray emission from the cluster consists of at least three discrete sources (Fig. 6); the apparently extended northern source, for example, may contain multiple point-like components and/or a substantial amount of enhanced diffuse emission in the vicinity. The spectra of these sources show the prominent K$\alpha$ emission lines of highly-ionized ions such as S XV, Ar XVII, Ca XIX and Fe XXV and are characterized by a two-temperature thermal plasma model of kT $\sim 1$ and 6 keV. Each source has an unabsorbed X-ray luminosity of $\sim 10^{35}$ ergs s$^{-1}$ in the 0.2–10 keV band. Portegies Zwart et al. (2001) have argued that such high-luminosity X-ray sources may still represent colliding wind binaries of extremely massive stars. However, the centroids of the X-ray sources don't match the positions of bright near-infrared stars, which typically have strong stellar winds (e.g., Cotera et al. 1996). Alternatively, the X-ray sources may represent emission peaks of the so-called cluster wind formed from the thermalization of colliding winds from a collection of individual stars (Raga et al. 2001).

But the diffuse X-ray emission from the vicinity of the cluster clearly has a different origin. The X-ray spectrum of the emission shows a strong 6.4-keV line with an equivalent width of $\sim 1$ keV (Yusef-Zadeh et al. 2002). We find that this K$\alpha$ emission of neutral to moderately-ionized irons is spatially correlated with a dense molecular cloud observed in the region. Therefore, the diffuse X-ray emission may primarily represent the scattered X-ray radiation from the cluster.

#### 3.1.2. Nonthermal Radio Filament

*Figure 7. X-ray contours overlaid on a 4.5 GHz radio continuum image of NTF G359.54+0.18 (Yusef-Zadeh 1997). The brightest point-like X-ray source in the field matches well spatially with a radio source.*

One of the most unique high-energy phenomena observed in the GC region is the presence of numerous nonthermal filaments (NTFs) of radio emission (Fig. 5). While the origin of these filaments remains largely unknown, finding an X-ray counterpart can provide important constraints on the particle energetics. We show in Fig. 7 a convincing association of an X-ray "thread" with NTF G359.54+0.18. This X-ray thread is about $1'$ long and has a width that is not adequately resolved on scales of $\sim 1''$. Interestingly, the X-ray emission is associated with the brightest of the two nearly parallel radio filaments and appears to have a flat spectrum, consistent with a nonthermal nature of the thread.

### 3.2. Large-scale diffuse X-ray emission

The high spatial resolution of the *Chandra* observations enables us, for the first time, to measure the diffuse X-ray component in the GC region with little contamination

*Figure 8. Diffuse X-ray emission across the X-ray spectrum: Red — 1–3 keV; Green — 3–5 keV; Blue — 5–8 keV. Source regions are replaced with interpolated values from surrounding regions. The resultant artifacts are apparent in regions around the two brightest sources 1E 1740.7-2942 and 1E 1743.1-2843. The images are adaptively smoothed with a Gaussian function to achieve a local count-to-noise ratio of* $\sim 8$*; much of the small-scale fluctuations is due to the Poisson noise.*

from discrete sources (Fig. 8). The presence of prominent line emission from ions such as S XV, Ar XVII, and Ca XIX (Fig. 4) in the diffuse X-ray spectrum indicates the presence

of gas at temperatures of $\sim 10^7$ K. The intensity image in the 1–3 keV band (Fig. 8), for example, is dominated by the line emission (Fig. 4), which traces the diffuse hot gas component. The emission is greatly enhanced in the recent star forming region close to Sgr A and the Radio Arc, where heating sources are abundant. The fast stellar winds from the three known young massive clusters alone (Galactic center, Arches, and Quintuplet; Figer et al. 1999), for example, account for a mechanical energy deposit of order $10^{39}$ ergs s$^{-1}$, comparable to that from the central cluster of the 30 Doradus nebula in the Large Magellanic Cloud (Wang 1999). The detectable lifetime of such clusters against the background star density is only a few megayears because of the strong gravitational tidal field in the GC region (Portegies Zwart et al. 2002). Therefore, the region may contain a lot of massive stars, which will end their life as supernovae, heating the ISM.

*Figure 9. 6.4-keV line intensity contours overlaid on the HCN* $J = 1 \rightarrow 0$ *emission (Jackson et al. 1996) from the central region of the Galaxy. The X-ray image is adaptively smoothed with a signal-to-noise ratio of* $\sim 3$*, after discrete sources with count rates greater than* $10^{-3}$ counts s$^{-1}$ *have been excised. A continuum contribution, estimated in the 4–6 keV and 7–9 keV bands, is subtracted.*

However, the overall spectrum of the diffuse X-ray emission (Fig. 4) appears substantially harder than expected for the thermal component alone. In fact, Fig. 8 shows that the observed X-rays in different energy bands often arise in different regions, indicating different origins. The prominent 6.4-keV line emission, for example, is probably not related directly to the thermal component. Part of the line emission is likely due to the fluorescent radiation from discrete sources, as in the case of the Arches cluster. Alternatively, the emission may be produced by the filling of K-shell vacancies produced by low-energy cosmic rays (Valinia et al. 2000). For both scenarios, one might expect a good correlation between the 6.4-keV emission and dense molecular gas tracers. However, such a correlation appears only globally, not on scales smaller than a few arcminutes (e.g., Fig. 9). This may indicate that the 6.4-keV emission is strongly influenced by local sources of hard X-ray radiation and/or low-energy cosmic rays.

Furthermore, we find that the emission distribution in the 4–6 keV band, where no prominent emission line is present, is substantially different from those of the above two emission lines, although differences in X-ray absorption are yet to be carefully considered. Most likely, the 4–6 keV band emission represents a combination of the thermal hot gas, scattered discrete source emission, and radiation from additional processes such as bremsstrahlung of nonthermal cosmic-ray electrons. The lack of enhanced X-ray emission from some of the most prominent nonthermal radio filaments and mid-infrared features indicates that the inverse Compton scattering of the cosmic microwave background or the interstellar infrared radiation is not a significant contributor to the observed diffuse X-ray emission.

Various radio studies have shown a global vertical configuration of inter-cloud magnetic fields, which extend to at least a few hundreds of pc away from the Galactic plane (e.g., LaRosa et al. 2000 and references therein). This configuration could result from vertical outflows of magnetized materials from the circumnuclear region (e.g., Wang et al. 2001). Indeed, the diffuse X-ray emission appears to extend beyond our surveyed field (Fig. 8). The outflow of the hot plasma and relativistic particles from the GC region may also be responsible for larger scale diffuse radio and soft X-ray features seen in the inner region of the Galaxy (Wang 1997; Almy et al. 2000; Sofue 2000).

*Figure 10. NGC 4631 as seen edge-on from the Chandra ACIS-S in the 0.3–1.5 keV band (shown in blue and purple color) and Ultraviolet Imaging Telescope (orange), tracing massive stars in the galaxy.*

*Figure 11. Central region of NGC 4631 in the Chandra ACIS-S 0.3–0.9 keV band (shown in blue and purple color), compared with a Hubble WFPC-2 Hα image (orange).*

## 4. Nearby Edge-on Galaxies

The best way to study the global galactic disk/halo interaction is to observe nearby edge-on galaxies. We have observed with the *Chandra* ACIS-S three nearby edge-on Scd galaxies as listed in Table 1. These galaxies, which show only little sign of nuclear starbursts, may be considered similar to our Galaxy in terms of morphology. Since they lie in directions of the sky with exceptionally low Galactic foreground absorption, they represent ideal cases to study their soft X-ray emission properties. Furthermore, while NGC 4631 is strongly interacting with a companion, NGC3556 is an isolated galaxy. The star forming rate in NGC 4244 is extremely low. The *Chandra* observations allow for comparison of the relative importance of galaxy-galaxy interaction and internal galactic activity in generating extraplanar hot gas.

*Figure 12. Optical image with overlaid radio continuum contours of NGC 3556 (King & Irwin 1997).*

We find only marginal evidence for diffuse X-ray emission in either the disk or the halo of NGC 4244. Both NGC 4631 and NGC 3556 show substantial diffuse soft X-ray emission beyond stellar disks (Wang et al. 2001; Figs. 10–11; Figs. 12–13). These observations provide the first unambiguous evidence for galactic coronae around galaxies that are similar to our Milky Way. The coronae morphologically resemble the radio halos of the galaxies (e.g., Fig. 13; Wang et al. 1995; Wang et al. 2001). One scenario for this radio-X-ray connection is that hot gas outflows are accompanied by magnetic field and cosmic rays and are confined ultimately by magnetic field at large galactic radius (Wang et al. 1995).

*Table 1. Parameters of Galaxies*[a]

| Parameter | NGC 4631 | NGC 3556 | NGC 4244 |
|---|---|---|---|
| Incl. angle (deg) | 85 | 86 | 90 |
| Distance (Mpc) | 6.9 | 11.6 | 3.1 |
| $L_{\rm FIR}/D_{25}^2$ | $3.5{\times}10^{40}$ | $3.2{\times}10^{40}$ | $0.29{\times}10^{40}$ |
| exposure (ks) | 60 | 60 | 50 |

[a]Parameters are obtained from Collins et al. (2000) and Hoopes & Walterbos. (1999). The mean surface far-infrared luminosity $L_{\rm FIR}/D_{25}^2$ is in units of ergs $s^{-1}$ $kpc^{-2}$.

The amount and extent of the extraplanar hot gas clearly depend on the star formation rate of a galaxy. For example, enhanced diffuse X-ray emission is apparently enclosed by numerous H$\alpha$-emitting loops blistered out from the central disk of NGC 4631, as is evident in a comparison with our deep Hubble Space Telescope imaging (Fig. 11; Wang et al. 2001).

*Figure 13. NGC 3556 across the Chandra ACIS-S spectrum: Red — 0.3–1.5 keV; Green — 1.5–3 keV; Blue — 3–7 keV. The radio contours are the same as in the previous figure.*

Expanding large-scale shell-like HI structures have also been found in both NGC4631 and NGC 3556 (Rand & van der Hulst 1993; King & Irwin 1997). These shells are very energetic; each requires an energy input equivalent to $\gtrsim 10^4$ SNe. Their nature is still a mystery. The two shells found in NGC 4631 are apparently associated with massive star forming regions, as traced by HII regions. Thus, the energy may be provided by numerous SNe and stellar winds from massive stars. Indeed, we find that two X-ray emission peaks spatially coincide with the shells. The peak associated with the eastern shell is extended and may represent hot gas within the shell. The X-ray emission from the western peak is, however, dominated by a bright point-like source, presumably an X-ray binary. Thus, high spatial resolution X-ray observations are essential for determining the nature of giant HI shells.

*Figure 14. Chandra ACIS-S image of NGC 4244 in the 0.3–1.5 keV band. The contours outline the morphology of the optical disk of the galaxy. The straight lines outline the boundaries of the X-ray data coverage.*

We find that the two partial HI shells (the so-called eastern and western features) identified by King & Irwin (1997) are not associated with any enhanced X-ray features. Therefore, these shells are probably not blown-out superbubbles produced by massive OB associations.

## 5. Summary

While our analysis of the *Chandra* observations described above is still ongoing, I summarize some of the preliminary results as follows:

- We have obtained the first arcsecond-resolution X-ray panorama of the GC region, which allows for direct comparison with similar maps in radio and infrared.
- We have detected about 1,000 discrete X-ray sources in the GC region. A substantial fraction of these sources are likely to be Galactic (e.g., massive stars and X-ray binaries).
- We find that the diffuse X-ray emission dominates over the contribution from faint discrete sources. The spectrum of the diffuse X-ray emission indicates the presence of large amounts of hot gas with temperatures of $\sim 10^7$ K. This hot gas originates in recent massive star

forming regions and possibly in the central black hole itself. There is evidence that the hot gas is escaping the regions into the Galactic halo. The outflow of the hot gas may be responsible for large-scale soft X-ray enhancements observed in the inner field of the Galaxy.
- The fluorescence and reflection of the radiation from discrete sources may be important in explaining the overall hard spectrum of the diffuse X-ray emission. One example is the X-ray emission from the surrounding region of the Arches cluster. The filling of K-shell vacancies produced by non-relativistic cosmic-rays may also be important in producing Fe K-shell vacancies.
- We have detected a giant corona around the edge-on disk galaxy NGC 4631 and a substantial diffuse extraplanar X-ray component in NGC 3556. The diffuse X-ray morphology of these galaxies resembles their radio halos, indicating a close connection between outflows of hot gas, cosmic rays, and magnetic fields from the galactic disks.
- The extraplanar diffuse X-ray-emitting gas evidently originates in star forming regions. In particular, enhanced X-ray emission is apparently enclosed by numerous H$\alpha$-emitting loops blistered out from the central disk of NGC 4631.

## References


Almy, R. C., McCammon, D. Digel, S.W., Bronfman, L., & May, J. 2000, ApJ, 545, 290

Baganoff, F., et al. 2001, Nature, 413, 45

Bregman, J. N., & Houck, J. C. 1997, ApJ, 482, 159

Collins, J. A., et al. 2000, ApJ, 536, 645

Cotera, A. S., et al. 1996, ApJ, 461, 750

Ebisawa, K., et al. 2001 , Science, 293, 1633

Figer, D., et al. 1999, ApJ, 525, 750

Hoopes, C. G., & Walterbos, R. A. M. 1999, ApJ, 522, 669

Jackson, J.M., Heyer, M. H., Paglione, T., & Bolatto, A. 1996, ApJL, 456, 91

King, D., & Irwin, J. A., 1997, New Astronomy, 2, 251

Koyama, K., et al. 1996, PASJ, 48, 249

LaRosa, T. N., et al. 2000, AJ, 119, 207

Portegies Zwart, S. F., et al. 2002, ApJ, 565, 265

Price, S. D., et al. 2001, ApJ, 121, 2819

Raga, A. C., et al. 2001, ApJL, 559, 33

Rand, R. J., & van der Hulst, J. M. 1993, AJ, 105, 2089

Sidoli, L., Belloni, T., & Mereghetti, S. 2001, A&A, 368, 835

Snowden, S. L., et al. 1997, ApJ, 485, 125

Sofue, Y. 2000, ApJ, 540, 224

Valinia, A., et al. 2000, ApJ, 543, 733

Wang, Q. D., et al. 1995, ApJ, 439,176

Wang, Q. D. 1997, in Lecture Notes in Physics 506, 503

Wang, Q. D. 1999, ApJL, 510, 139

Wang, Q. D., et al. 2001, ApJL, 555, 99

Wang, Q. D., Gotthelf, E. V., & Lang, C., 2002, Nature, 415, 148

Yusef-Zadeh, F., Wardle, M., & Parastaran, P. 1997, ApJ, 475, 119

Yusef-Zadeh, F., et al., 2002, ApJ, in press, astro-ph/0108174


## Acknowledgements


I thank my collaborators for their contributions to the work described above and acknowledge the support from NASA/CXC through grants, GO0-1150, GO0-1095, GO1-2084, and GO1-2150.

This figure "qwang-E3_fig1.jpeg" is available in "jpeg" format from:

http://arXiv.org/ps/astro-ph/0202317v1

This figure "qwang-E3_fig2.jpeg" is available in "jpeg" format from:

http://arXiv.org/ps/astro-ph/0202317v1

This figure "qwang-E3_fig3.jpeg" is available in "jpeg" format from:

http://arXiv.org/ps/astro-ph/0202317v1

This figure "qwang-E3_fig5.jpeg" is available in "jpeg" format from:

http://arXiv.org/ps/astro-ph/0202317v1

This figure "qwang-E3_fig6.jpeg" is available in "jpeg" format from:

http://arXiv.org/ps/astro-ph/0202317v1

This figure "qwang-E3_fig7.jpeg" is available in "jpeg" format from:

http://arXiv.org/ps/astro-ph/0202317v1

This figure "qwang-E3_fig8.jpeg" is available in "jpeg" format from:

http://arXiv.org/ps/astro-ph/0202317v1

This figure "qwang-E3_fig9.jpeg" is available in "jpeg" format from:

http://arXiv.org/ps/astro-ph/0202317v1

This figure "qwang-E3_fig10.jpeg" is available in "jpeg" format from:

http://arXiv.org/ps/astro-ph/0202317v1

This figure "qwang-E3_fig11.jpeg" is available in "jpeg" format from:

http://arXiv.org/ps/astro-ph/0202317v1

This figure "qwang-E3_fig12.jpeg" is available in "jpeg"  format from:

http://arXiv.org/ps/astro-ph/0202317v1

This figure "qwang-E3_fig13.jpeg" is available in "jpeg" format from:

http://arXiv.org/ps/astro-ph/0202317v1

This figure "qwang-E3_fig14.jpeg" is available in "jpeg"  format from:

http://arXiv.org/ps/astro-ph/0202317v1